

# Evaporation Channel as a Tool to Study Fission Dynamics

A. Di Nitto,<sup>1,2,\*</sup> E. Vardaci,<sup>1,3</sup> G. La Rana,<sup>1,3</sup> P. N. Nadtochy,<sup>1,4</sup> and G. Prete<sup>5</sup>

<sup>1</sup>*Istituto Nazionale di Fisica Nucleare, Sezione di Napoli, 80126 Napoli, Italy*

<sup>2</sup>*Johannes Gutenberg-Universität Mainz, 55099 Mainz, Germany*

<sup>3</sup>*Dipartimento di Fisica, Università degli Studi di Napoli "Federico II", Italy*

<sup>4</sup>*Omsk State Technical University, Mira prospekt 11, 644050 Omsk, Russia*

<sup>5</sup>*Laboratori Nazionali di Legnaro dell'Istituto Nazionale di Fisica Nucleare, 35020 Legnaro (Padova), Italy*

(Dated: March 22, 2022)

The dynamics of the fission process is expected to affect the evaporation residue cross section because of the fission hindrance due to the nuclear viscosity. Systems of intermediate fissility constitute a suitable environment for testing such hypothesis, since they are characterized by evaporation residue cross sections comparable or larger than the fission ones. Observables related to emitted charged particle, due to their relatively high emission probability, can be used to put stringent constraints on models describing the excited nucleus decay and to recognize the effects of fission dynamics. In this work model simulations are compared with the experimental data collected via the  $^{32}\text{S} + ^{100}\text{Mo}$  reaction at  $E_{\text{lab}} = 200\text{ MeV}$ . By comparing an extended set of evaporation channel observables the limits of the statistical model and the large improvement coming by using a dynamical model are evidenced. The importance of using a large angular covering apparatus to extract the observable is stressed. The opportunity to measure more sensitive observables by a new detection device in operation at LNL are also discussed.

PACS numbers: 27.60.+j; 25.70.Jj; 24.60.Dr; 24.75.+i; 29.40.-n

## I. INTRODUCTION

Since the discovery of nuclear fission in 1939 [1, 2] a large effort was devoted to provide a realistic description of this complex phenomenon originated by the interplay of macroscopic and microscopic degrees of freedom in a nucleus. With the advent of heavy-ion accelerators the study of fission was extended to a new variety of nuclei produced in few-nucleon direct transfer reactions [3, 4] or in complete fusion reactions (as in recent works [5, 6]). More recently by using reactions with radioactive beams it was demonstrated that fission studies can be performed also on very neutron-deficient mercury-to-thorium nuclei [7].

It is well established that fission is a slow process dominated by nuclear viscosity. A very striking experimental evidence of this behaviour is the excess of pre-scission light particles, with respect to the predictions of the statistical model (SM), and its dependence on the excitation energy [8]. Phenomenological studies based on the SM predictions were carried out with the aim to estimate the fission delay time, and, in some cases, extract the strength of nuclear viscosity. The estimates given by different authors predict a quite wide range of dissipation strengths and different dependencies on temperature and deformation (see reviews [9–11] and references therein). However, this kind of approach is founded on the reliability of the SM to reproduce the observables in the evaporation residue (ER) channel, and this has not yet been fully explored.

The lack of experimental constraints to the model appears to be, in several cases, one of the source of controversial results. By considering large set of observables the limits of the SM have been evidenced [12, 13]. Dynamical models based

on a stochastic approach combined with an evaporative model, for light particles and gamma quanta, seem to be a more suitable tool for the description of the collective evolution of nuclei [14, 15]. Although much work has been devoted to fission dynamics, there are still many open questions: the time-scale, the strength and nature of dissipation, as well as the dependence on the temperature and shape of the fissioning system are key items still to be disentangle.

The dynamics of the fission process is expected to affect the evaporation residue channel because of the fission hindrance due to nuclear viscosity. Systems of intermediate fissility constitute a suitable environment for measuring potentially informative observables, being characterized by higher probability for charged particle emissions and integral ER cross section comparable with the fission one. In order to address fission dynamics such advantages were largely exploited by using as probes the light particles [16] and, only recently, by using the fission-fragment charge distribution [17]. However in order to fruitfully benchmark the existing models the experimental uncertainties have to be minimized, thereby larger angular coverage apparatuses are essential to step forward.

Here we report on the measurement and analysis of the evaporation and fission decay of the compound nucleus  $^{132}\text{Ce}$  at  $E_x = 122\text{ MeV}$ , produced by the  $200\text{ MeV } ^{32}\text{S} + ^{100}\text{Mo}$  reaction. For this system ER and fusion fission (FF) angular distributions and cross sections, light charged particle (LCP) multiplicities and spectra as well as ER-LCP angular correlations were measured [12, 18]. The measured quantities were compared with the SM calculations carried out by changing many physical ingredients of the model as well as with a dynamical model based on the 3-D Langevin equations. It was found that the ER observables, especially the LCP multiplicities and ER-LCP angular correlations, can be used not only to fix SM parameters, but also to provide constraints on the ingredients describing the fission mechanism. The analysis

\* corresponding author e-mail: a.dinitto@gsi.de

based on the dynamical model, i.e. considering a more realistic approach [18], shows better data reproduction. However there is still substantial room for improving the reliability of such conclusions. One mean is to investigate what observables can be still identified to be affected by fission dynamics. Additional observables with such properties are for example the partial multiplicities and ER-LCP correlation angular distribution as function of evaporation residues angles that can be measured by coupling the new PPAC recently used at LNL [19] and the  $8\pi$ LP detection apparatus.

This article is organized as it follows. In Sec. II we present in more detail the description of the experimental setup. In Sec. III the theoretical models used for simulations are briefly introduced. In Sec. IV we show the observables that provide benchmarks for parameters and prescriptions describing the fission dynamics. We first discuss the result of comparison between experimental data and simulations and afterwards the advantages offered by using a recently developed detection setup. In Sec. V we draw our conclusions.

## II. EXPERIMENTAL SETUP

The experiment was performed at the Tandem accelerator of Laboratori Nazionali di Legnaro. A pulsed beam of  $^{32}\text{S}$  of intensity of about 1-3 nA was used to bombard a self-supporting  $^{100}\text{Mo}$  target  $400 \mu\text{g}/\text{cm}^2$  thick. A beam burst with period of 800 ns and duration of about 3 ns was used.

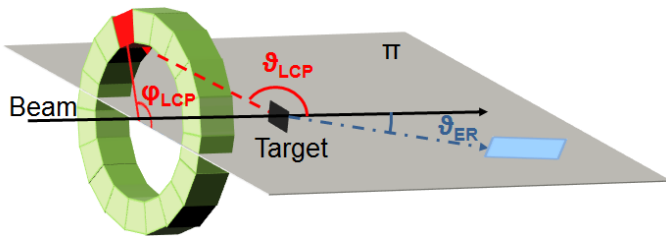


FIG. 1. (Color online) Schematic presentation of a coincident event where the LCP is detected by a Ball telescope and ER by a PPAC. The emission angle of evaporation residue ( $\theta_{\text{ER}}$ ) is included between the beam direction and the line connecting the center of PPAC and the target. These two lines define the reaction plane  $\pi$ . The polar and azimuthal angles ( $\theta_{\text{LCP}}$ ) and ( $\phi_{\text{LCP}}$ ), respectively, define the direction of LCP impinging on a Ball telescope. A Ring at ( $\theta_{\text{LCP}}$ ) is shown. It is made of 18 identical telescopes mounted at same polar angle and spanning all the possible azimuthal directions.

We used the Ball sector of  $8\pi$ LP apparatus [20] to detect light charged particles and fission fragments, while the heavy residues were detected in a system of four parallel plate avalanche counters (PPAC) placed at forward angles. The Ball, covering the polar angle from 34 to 165 degrees, has a diameter of 30 cm and consists of 7 rings of  $\Delta E$ -E telescopes placed co-axially around the beam direction. The schematic of one backward ring is shown in Fig. 1. Each ring contains 18 telescopes. Each telescope points towards the center of the target, and covers a polar angular opening of 17 degrees. Considering this geometry, the detectors in a ring have the

same average polar angle with respect to the beam direction axis, and all together they cover the azimuthal angle from 0 to 360 degrees. As a whole the Ball covers a solid angle of about 80% of  $4\pi$  by means of 125 telescopes. Each telescope is made by a first stage ( $\Delta E$ ) of  $300 \mu\text{m}$  thick Si detectors followed by a second stage (E) of 5 mm thick CsI(Tl) with photodiode read out. Particle identification was carried out by using the  $\Delta E$ -E technique for the particles that have energy enough to pass through the  $\Delta E$  stage and Pulse Shape Discrimination for those stopping in the Si detectors. During the experiment identification thresholds of 0.5 MeV for protons and 1 MeV for  $\alpha$  particles were obtained. The four PPAC modules were placed symmetrically with respect to the beam direction to measure evaporation residues. Each PPAC module consists of two coaxial PPACs (front and rear) operating in the same gas volume at the pressure of about 40 Torr and mounted at the distance of 15 cm from each other. This gas pressure was sufficient to stop the ER between the two PPACs, and let the other ions, like FF and elastic scattered beam particles, reach the rear PPAC. ERs are therefore selected by a vetoed Time of Flight technique: the time between the beam RF signal and the signal from the front PPAC is recorded only if the signal from the rear PPAC is missing. This method allows to reject, with high efficiency, signals due to ions reaching the rear PPAC which are much faster and much lighter than evaporation residues. Each PPAC module was positioned at 4.5 degrees with respect to the beam direction and subtended a solid angle of 0.8 msr.

Data were collected by requiring several triggering conditions, as described in [12], to perform measurements of the single and coincidence yields in the same run. In this way an extended set of observables relative to the fusion-evaporation channel was obtained that consists of proton and  $\alpha$  particle multiplicities and energy spectra, as well as angular correlations among the LCP and ER. The angular distribution of evaporation residues was obtained by means of the electrostatic deflector PISOLO [21] in a complementary experiment as described in details in ref.[12]. The experimental data will be shown in section IV.

## III. MODELS

The extended set of observables, collected as described above, was compared with the predictions provided by the SM code PACE2\_N11 and a dynamical model. The computer code PACE2\_N11 is an extensively modified version of the code PACE2 [22] that simulates the multistep deexcitation of the compound nucleus both through light particle evaporation and fission. Light particle evaporation is implemented according to the Hauser-Feshbach formulation and the fission probability is calculated by using the transition-state model. Fission barriers are computed with the Finite Range Liquid Drop Model (FRLDM) [23]. The competition between the different decay modes is treated with a Monte Carlo approach. PACE2 was modified to implement options for leading parameters (transmission coefficients, level density parameter and yrast line) and to take into account the fission delay time  $\tau_d$

[12, 13, 24, 25]. In particular, the fission decay width is given by the following formula:

$$\Gamma_f = f(t)\Gamma_{BW} \quad (1)$$

where  $f(t)$  is a simple step function:  $f(t) = 0$  for  $t < \tau_d$  and  $f(t) = 1$  for  $t > \tau_d$ .  $\Gamma_{BW}$  is the Bohr-Wheeler width [26].

In the dynamical model [14, 18] the fission process is described with a stochastic approach code based on 3-D Langevin Equations combined with the computer code LILITA\_N11 [27] to simulate the evaporation of LCP. The nuclear shapes are described by  $(c, h, \alpha)$  parametrization [28], related to the collective variables which give the evolution of fissioning nuclei:  $(c)$  elongation,  $(h)$  neck size at given  $c$  and  $(\alpha)$  mass asymmetry. The use of LILITA\_N11 allows to adopt the same options for leading parameters implemented in PACE2\_N11.

Both codes were modified in order to produce an event-by-event output of emitted ER and light particles that, filtered according to the response function of  $8 \pi LP$ , can be used for a direct comparison of predictions and experimental data.

#### IV. RESULTS AND DISCUSSION

The main goal of this analysis is to exploit the evaporation channel observables in order to put stringent constraints on the SM parameters included in the models used for fission dynamics studies. These parameters are also used to describe the evaporation of light pre-scission particles emitted by the compound nucleus along the path from its formation up to the scission in two fragments. This study will not solve the existing ambiguity concerning the ingredients describing the dynamical evolution of fissioning systems, as mass and friction [15], but at least can avoid that they will be affected by the incorrect definition of the SM parameters, as discussed in [18].

In a previous work the  $^{32}\text{S} + ^{100}\text{Mo}$  reaction at 200 MeV extended data set was compared with SM calculations[12]. In such work it was observed that if the analysis is limited to the pre-scission LCP multiplicities and FF cross section, as usually done in fission dynamics studies [29], can be reasonably well reproduced without any delay. From this result one could conclude that no dynamical effects take place in the decay of CN. However different combination of the input parameters does not exclude the presence of a relatively small fission delay, as expected by the systematics [30]. On the other hand, a model, that strongly overestimates the ER particle multiplicities, cannot be considered reliable to estimate the fission time-scale through the pre-scission LCP multiplicities. Therefore we used the ER angular distributions and LCP evaporative spectra to limit the SM parameters included in the dynamical model. Calculations considering different dissipation mechanisms were compared with the full set of experimental data and most of the observables were well reproduced [18, 31]. Therefore the ingredients describing the fission process were determined.

In this section the data are presented in a way to progressively show the impact of SM parameters on different observ-

ables. Finally the advantages coming by using a new detection system for ERs in operation at LNL, will be illustrated in the light of model predictions.

The importance to explore very selective observables will be evidenced in the comparison with existing data and the importance of new observables will be illustrated by comparing simulations filtered with the new detection system geometry.

#### A. Evaporation residue angular distributions and evaporative LCP energy spectra

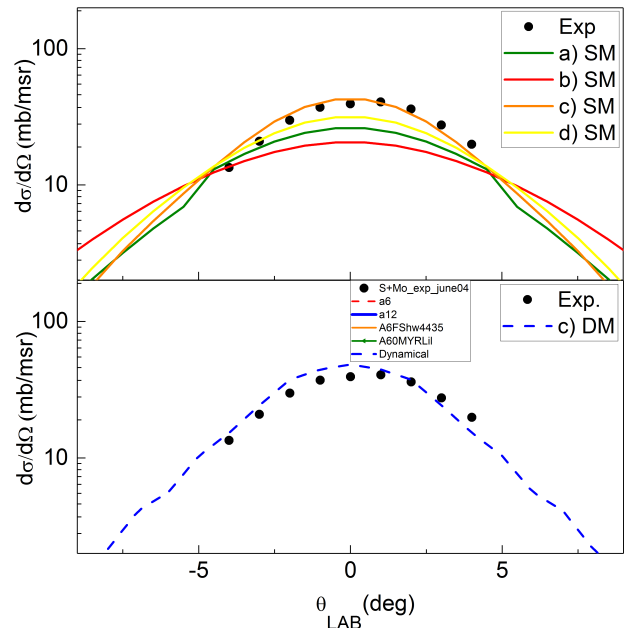


FIG. 2. (Color online) ER angular distribution of the reaction  $^{32}\text{S} + ^{100}\text{Mo}$ . The experimental data (dots) are compared with the SM calculations (top) performed with the four prescription of Tab. I and with dynamical model calculation (bottom) performed by using only the prescription (c).

In Fig. 2 we show the angular distribution of the evaporation residues compared with the results of the statistical model and the dynamical model calculations. The experimental statistical errors are in the order of the point size. By changing the leading parameters of the SM significant deviations are produced in the ER angular distributions as shown in Fig. 2a. The leading parameters of the simulations were the LCP transmission coefficients, the level density parameters  $a$ , for particle evaporation, and the yrast line prescriptions. Transmission coefficients derived from the optical model (OM) [32–34] and from the fusion systematics (FS) [35] in combination with a level density parameters between  $A/6$  and  $A/12$  were used. The moment of inertia was calculated by adopting prescriptions for the yrast line with parameters from the Rotating Liquid Drop Model (RLDM) [23] or by assuming the compound nucleus as a the rigid sphere (RS) with  $r_0 = 1.2$  fm.

The four different prescriptions used in the simulations

| Prescriptions | $a_v$ | Yrast Line | Trans. Coef. |
|---------------|-------|------------|--------------|
| a)            | A/6   | RLDM       | OM           |
| b)            | A/12  | RLDM       | OM           |
| c)            | A/6   | RS         | FS           |
| d)            | A/6   | RS         | OM           |

TABLE I. Prescriptions of SM parameter set adopted in the calculations for 200 MeV  $^{32}\text{S} + ^{100}\text{Mo}$  reaction.

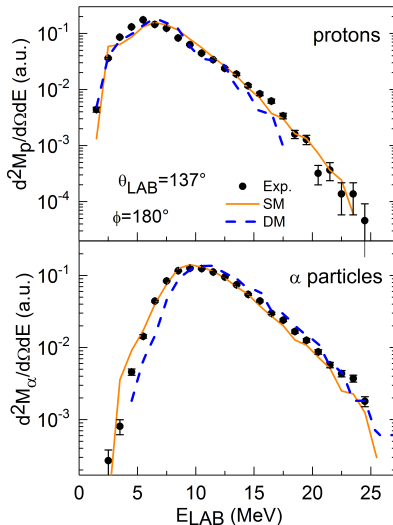


FIG. 3. (Color online) Proton (top) and  $\alpha$  particle (bottom) energy spectra measured in coincidence with ERs. The experimental data (dots) are compared with the predictions of the statistical model (solid line) and the dynamical model (dashed line).

shown in Fig. 2a are reported in Tab. I. They were chosen among many combinations of the SM parameter values. The aim was to explore the full range of variability of the observables under examination. No fission delay was included in the calculations and the ratio  $a_f/a_v$  was kept equal to 1 due to relatively weak effects on the ER observables (see discussion in [12]). The comparison of ER angular distributions in Fig. 2a shows that the data are not well reproduced with a), b) and d) prescriptions, whereas a reasonable good agreement can be obtained by adopting the c) prescription. The dynamical and the statistical models adopt different approaches to take into account fission-evaporation competition, however it was observed that, if the SM parameters of c) prescription are used, the data can be reproduced with comparable accuracy by both models, as shown in Fig. 2b for the DM. Therefore the c) prescription was used in both models in the following comparisons with the other experimental data.

In Fig. 3 the measured evaporative proton and  $\alpha$  particle energy spectra are compared with results of statistical and dynamical model simulations. Both models very well reproduce the proton spectrum and the high energy side of  $\alpha$  particle spectrum, whereas the low energy side of this latter is better reproduced with the SM. The same agreement holds also for the spectra measured at different angles. Therefore it is reasonable to conclude that an overall agreement of energy spec-

tra and angular distributions of evaporation residues can be obtained by adopting both the SM and the DM. The use of the other prescriptions in Tab. I produce large deviations not only in the evaporation residues distribution, but also in the energy spectra (for details see [12]). The sensitivity reachable in this comparison can provide indications for the most appropriate SM parameters needed to describe the evaporation channel, but it is not sufficient to distinguish which model better reproduces the experimental data, being the observable so far considered only slightly influenced by the evaporation-fission competition.

## B. LCP multiplicities

The LCP differential multiplicities were obtained by normalizing the  $8\pi$ LP Ball-PPAC coincidence yields to the number of the ER events and then divided by the LCP detector solid angle. The resulting differential multiplicities of LCP

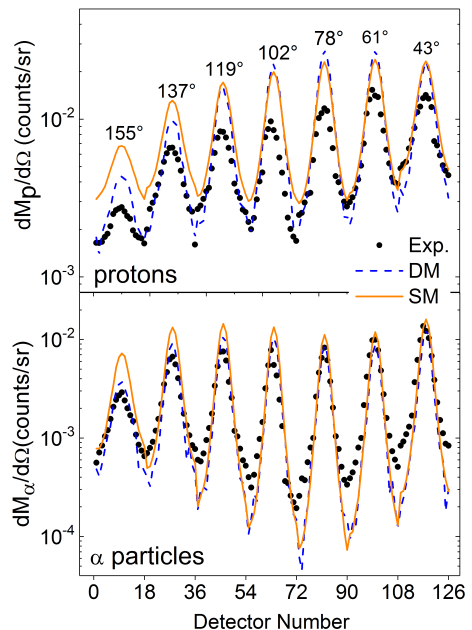


FIG. 4. (Color online) Experimental and calculated protons (top) and  $\alpha$  particles (bottom) differential multiplicity distributions as function of  $8\pi$ LP Ball detector identification number. Black dots represent the experimental data, whereas the blue and orange lines are the SM and DM simulations, respectively. See the text for details.

are shown in Fig. 4 as a function of the Ball detector number, starting from the most backward angles. As mentioned before, for a fixed polar angle, the telescopes span the azimuthal angle from  $0^\circ$  to  $360^\circ$ . The oscillating behavior as function of the detector number is due to a combined effect of kinematics and of angular momentum of the composite system. In particular, the maxima correspond to events where ERs and LCPs are emitted in-plane and on opposite side with respect to the beam direction,  $\phi_{\text{LCP}} = 0^\circ$ , whereas the minima occur when ERs and LCPs are emitted in-plane but on the same side

|      | $M_p$           | $M_\alpha$      | $\sigma_{ER}$ | $\sigma_{FF}$ |
|------|-----------------|-----------------|---------------|---------------|
| DM   | 1.20            | 0.56            | 793           | 143           |
| SM   | 1.43            | 0.72            | 817           | 139           |
| Exp. | $0.90 \pm 0.14$ | $0.56 \pm 0.09$ | $828 \pm 50$  | $130 \pm 13$  |

TABLE II. The experimental and calculated mean particle multiplicities in the ER channel together with the fission and evaporation cross sections.

with respect to the beam direction, i.e.  $\phi_{LCP} = 180^\circ$ . In the figure the mean polar angles corresponding to the telescope detecting the LCP,  $\theta_{LCP}$ , are indicated. By adopting different SM parameters the differential LCP multiplicities, and in particular those relative to the  $\alpha$  particle distributions, will be largely affected not only in terms of the bulk shapes ( see for instance the changing in the maxima to minima ratios in [12]), but also in terms of absolute values. The experimental data are compared with the results of the SM and DM calculations assuming the c) prescription and without relative normalization. The data seem to be better reproduced by the DM simulation being characterized by slightly smaller maxima. Looking the data in Tab. II this is mainly true for protons.

By using the SM a consistent overestimation of both LCP multiplicities in the evaporation channel can be evidenced, while the evaporation and fission cross sections are well reproduced, see Tab. II. The DM predicts not only evaporation and fission cross sections consistent with the experimental data, but also the evaporative  $\alpha$  particle multiplicity; only the proton multiplicity is slightly overestimate. Therefore by using the DM is possible to obtain a good overall agreement in the evaporation channel that makes us confident on the use of such model for studying fission process [18].

### C. New Observables

High precision measurements of the evaporative LCP absolute multiplicities can be obtained only by measuring simultaneously ERs and LCPs emitted on the full solid angle. However, the experimental apparatuses have limited angular coverages and only partial multiplicities are accessible. For this reason the absolute multiplicities, as those reported in Tab. II, are not directly measured, but are extracted being driven by model predictions. The use of 4 symmetric PPACs positioned at 4.5 degrees around the beam direction is convenient because it allows to perform redundant measurements. The redundancy is very useful because from one side assures the correct alignment of the beam impinging on the target, and from the other allows to apply the summing procedure to reduce statistical fluctuations. By using our setup the partial multiplicities were obtained as the ratios among the yields of LCP in coincidence with ER's and the yields of all ER's detected by our PPAC's. Afterward, the absolute multiplicities were estimated by considering the simulated ratios among the angle-integrated multiplicities and the quantity obtained by filtering the event by event output of the simulation code considering the geometry of the  $8\pi$ LP apparatus and the old PPAC system mounted at 4.5 degrees. The ratios obtained were  $1.3 \pm 0.2$  for pro-

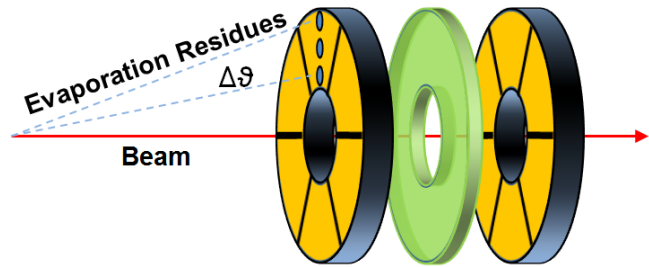


FIG. 5. Exploded view of the new PPAC system for evaporation residue detection. This system can be combined with mask to measure ions emitted at around the forward direction at different polar angles,  $\theta_{ER}$ , by spanning the  $\Delta\theta$  angular range.

tons and  $1.7 \pm 0.3$  for  $\alpha$  particles, therefore the reported errors take into account the wider variability produced by changing SM parameters in both PACE2\_N11 and LILITA\_N11 simulations. Therefore to reduce the uncertainties and benchmark the fission models an experimental technique able to exclude the model dependence of observables is needed.

The large angular coverage offered by the  $8\pi$ LP array can indeed favor the search for additional observables affected by the channel's competition in the CN decay process. It was shown before that the reproduction of energy spectra and angular distributions of evaporation residues do not guarantee a good reproduction of the full de-excitation process. Because of this we extracted the differential multiplicities, which are simultaneously influenced by evaporation residues and LCP angular distributions and the competition with the fission channel over the extended  $8\pi$ LP angular range, and it was directly compare with the simulations in order to identify the most suitable SM parameters. In order to further exploit this concept, we have built a new PPAC system to detect evaporation residues at the most significant forward angles for fusion reactions.

The new system for ER detection, whose schematic is shown in the Fig. 5, consists of two annular PPACs (front and rear) divided in 6 independent sectors with a wide area and an absorber foil mounted in between. The absorber is adapted to the experimental conditions with thickness sufficient to stop only ERs and to let the other lighter ions, like LCPs and elastic scattered beam particles, passing through and reach the rear PPAC. The ERs are therefore selected using as a veto the rear PPAC signal. In the previous experiment by using this system we were able to measure also the time of flight of ERs and improve the selectivity by excluding those produced by the beam interaction with target backing material. To detect ER angular distribution between 3 and 8 degrees with respect to the beam a mask was mounted in front of the PPAC as indicated by the three blue spots in the Fig. 5. Furthermore it should be underlined that thanks to the symmetric arrangement of the Ball telescopes and the PPAC sectors, also with this system it is possible to perform redundant measurements and get the consequent benefits.

The experimental point of the ratio between the  $\alpha$  particle and proton partial multiplicities measured with the old PPAC

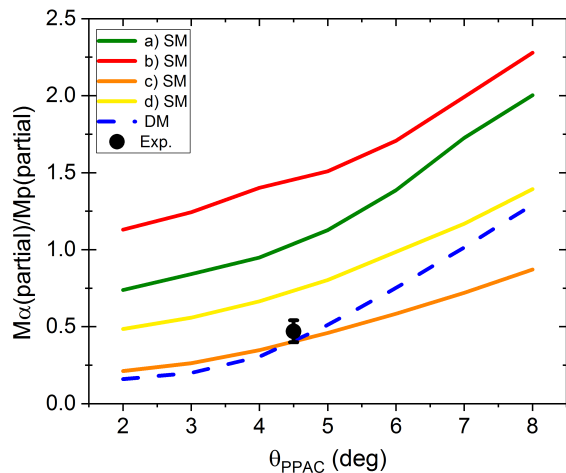


FIG. 6. (Color online) Ratios between  $\alpha$  particles and protons partial multiplicities obtained with  $8\pi$ LP Ball filter as function of ER detection angles. The lines represent the SM calculations performed by using the four prescriptions of Tab. I and the DM calculation, the dot is the experimental value measured with  $8\pi$ LP Ball and the PPAC at 4.5 degrees.

system mounted at 4.5 degrees is shown in the Fig. 6. This quantity has the advantage to be at same time model independent and very sensitive not only to the decay kinematic, but also to the competition between evaporative LCP and fission channels. Therefore we compared the experimental data point with simulations obtained by using the four prescriptions of Tab. I in PACE2\_N11 and the dynamical model. In order to have a more general view of the behaviour, we simulate the trend of partial multiplicities by considering the different geometrical selections that can be applied by using the new PPAC, i.e. the measure of ER emitted at different mean angles ( $\theta_{\text{PPAC}}$ ). The ratios of partial multiplicities as function of  $\theta_{\text{PPAC}}$  appear to be a good probe, as they are very sensitive to the SM parameters. In general it is possible to observe a reduction of the proton partial multiplicities with the increase of  $\theta_{\text{ER}}$ , on the contrary the  $\alpha$  particle multiplicities quickly increase. This behaviour can be explained by considering that ERs at larger  $\theta_{\text{ER}}$  need more recoil that is preferably provided by  $\alpha$  particle evaporation. Therefore the  $\alpha$  particle multiplicities increase. However  $\alpha$  emission removes more excitation energy with respect to lighter particles, and the probability of a coincident proton emission will be reduced further increasing the ratio at high  $\theta_{\text{ER}}$ . More complicated is to explain the differences originated by each single SM parameters. For a fixed yrast line, increasing  $a$ , produces almost constant reduction in the ratios (see the prescriptions a) and b)). Going from the yrast line calculated using the RLDM to the yrast line assuming the nucleus as a rigid sphere with  $r_0 = 1.2$  fm, that means a decrease of the moment of inertia, we observe a decrease in the ratios, that becomes larger with  $\theta_{\text{PPAC}}$  (see the prescriptions a) and d)). While by changing transmission coefficients, i.e. passing from OM to FS ones, there is a decrease of about a factor two in the ratio that is almost independently from the ER angles considered, (see prescription c) and d)).

We observed that only combining all the effects producing a decrease in the  $\alpha$  particle to proton multiplicity ratios is possible to improve the reproduction of experimental data, and, in agreement with all the other observables, the prescription c) is the best set of parameters. By comparing the statistical model calculation with the dynamical one, only small differences are observed at  $\theta_{\text{PPAC}} = 4.5$  degrees that cannot provide a conclusive indication about which of the two models better describe the CN decay. However, the differences become larger and larger by increasing the  $\theta_{\text{ER}}$ . Therefore we planned to measure these observables as function of evaporation residue angles by coupling the  $8\pi$ LP detection apparatus and the new PPAC system. Such very promising measurements highlight once more how the investigation of evaporation channel can play a relevant role in fission dynamic studies, in fact the reduction of the uncertainties on very exclusive observables can provide strong constraints not only to optimize the SM parameters, but also to validate the existing models.

## V. SUMMARY AND CONCLUSIONS

The high charged particle multiplicities in pre-scission and evaporation channels existing in the intermediate fissility composite systems, makes them a good probe to get information on the fission process. In this work we studied the evaporative light charged particles emitted by the  $^{132}\text{Ce}$  nuclei at  $E_x = 122$  MeV by comparing the simulations with experimental data measured with the  $8\pi$ LP apparatus. The simulations were performed using the SM code PACE2\_N11 and a dynamical model based on the 3-D Langevin equations.

Evaporation residue angular distribution and LCP energy spectra were used to define the SM parameters included for SM and DM simulations. By using the PACE2\_N11 code, irrespective of the SM parameters adopted, the evaporative  $\alpha$  particle and proton multiplicities are overestimated. Such a failure would affect also the emission probability in the pre-scission channel, making the extraction of the fission delay time unreliable. Better results can be obtained by using the DM the evaporative LCP multiplicities which are reasonably well reproduced. This indicates that extended data set are essential to define simulations that can be considered reliable in order to address the open questions on fission dynamics.

Detailed studies evidenced the high sensitivity of LCP differential multiplicities not only to the SM parameters, but also to the nuclear shapes [19]. The DM reproduces better also these observables, however not very large differences exist with respect to the SM predictions. The main limitation to put stringent bounds on the SM parameters can be attributed to the uncertainties on experimental data, which are still slightly model dependent. Therefore in order to increase the sensitivity we plan to measure in future experiments observables where particle and evaporation residue angular distributions are combined. The possibility to use detection setup with a larger angular coverage clearly represent a significant advance to benchmark the fission models, and in conjunction with recent theoretical developments [15] should act as a spur for

future measurements in this field. By means of an annular PPAC the angular distribution of the ratios between the  $\alpha$  particle and proton partial multiplicities can be measured over an extended angular coverage. This quantities have smaller uncertainties, being model independent, and according the predictions it is extremely sensitive not only to the main (lead-

ing) evaporative parameters, but also to the fission process description included in the statistical and the dynamical model adopted in this work. In conclusion, the model strongly indicate that the exclusive observables of evaporation channel represent a powerful tool to define the fission dynamics that have to be considered in future studies.

- 
- [1] L. Meitner and O. R. Frisch, *Nature* **143**, 239 (1939).
- [2] O. Hahn and F. Strassmann, *Naturwissenschaften* **27**, 11 (1939).
- [3] A. Saxena, D. Fabris, G. Prete, D. V. Shetty, G. Viesti, B. K. Nayak, D. C. Biswas, R. K. Choudhury, S. S. Kapoor, M. Barbui, E. Fioretto, M. Cinausero, M. Lunardon, S. Moretto, G. Nebbia, S. Pesente, A. M. Samant, A. Brondi, G. La Rana, R. Moro, E. Vardaci, A. Ordine, N. Gelli, and F. Lucarelli, *Phys. Rev. C* **65**, 064601 (2002).
- [4] R. Léguillon, K. Nishio, K. Hirose, H. Makii, I. Nishinaka, R. Orlandi, K. Tsukada, J. Smallcombe, S. Chiba, Y. Aritomo, T. Ohtsuki, R. Tatsuzawa, N. Takaki, N. Tamura, S. Goto, I. Tsekhanovich, C. Petrache, and A. Andreyev, *Physics Letters B* **761**, 125 (2016).
- [5] J. Khuyagbaatar, D. J. Hinde, I. P. Carter, M. Dasgupta, C. E. Düllmann, M. Evers, D. H. Luong, R. du Rietz, A. Wakhle, E. Williams, and A. Yakushev, *Phys. Rev. C* **91**, 054608 (2015).
- [6] E. M. Kozulin, E. Vardaci, I. M. Harca, C. Schmitt, I. Itkis, G. Knyazheva, K. Novikov, A. Bogachev, S. Dmitriev, T. Loktev, F. Azaiez, I. Matea, D. Verney, A. Gottardo, O. Dorvaux, J. Piot, G. Chubarian, W. H. Trzaska, F. Hanappe, C. Borcea, S. Calinescu, and C. Petrone, *The European Physical Journal A* **52**, 293 (2016).
- [7] A. N. Andreyev, M. Huyse, and P. Van Duppen, *Rev. Mod. Phys.* **85**, 1541 (2013).
- [8] D. J. Hinde, D. Hilscher, H. Rossner, B. Gebauer, M. Lehmann, and M. Wilpert, *Phys. Rev. C* **45**, 1229 (1992).
- [9] D. Hilscher and H. Rossner, *Ann. Phys. Fr.* **17**, 471 (1992).
- [10] P. Fröbich and I. Gontchar, *Physics Reports* **292**, 131 (1998).
- [11] E. Vardaci, A. Di Nitto, P. N. Nadtochy, A. Brondi, G. La Rana, R. Moro, M. Cinausero, G. Prete, N. Gelli, E. M. Kozulin, G. N. Knyazheva, and I. M. Itkis, *Pramana Journal of Physics* **82**, 345 (2015).
- [12] A. Di Nitto, E. Vardaci, A. Brondi, R. La Rana, G. and Moro, P. N. Nadtochy, M. Trotta, A. Ordine, A. and Boiano, M. Cinausero, E. Fioretto, G. Prete, V. Rizzi, D. V. Shetty, M. Barbui, D. Fabris, M. Lunardon, G. Montagnoli, S. Moretto, G. Viesti, N. Gelli, F. Lucarelli, G. N. Knyazheva, and E. M. Kozulin, *The European Physical Journal A* **47**, 83 (2011).
- [13] E. Vardaci, A. Di Nitto, A. Brondi, G. La Rana, R. Moro, P. N. Nadtochy, M. Trotta, A. Ordine, A. Boiano, M. Cinausero, E. Fioretto, G. Prete, V. Rizzi, D. Shetty, M. Barbui, D. Fabris, M. Lunardon, G. Montagnoli, S. Moretto, G. Viesti, N. Gelli, F. Lucarelli, G. N. Knyazheva, and E. M. Kozulin, *The European Physical Journal A* **43**, 127 (2010).
- [14] P. N. Nadtochy, E. Vardaci, A. Di Nitto, A. Brondi, G. La Rana, R. Moro, M. Cinausero, G. Prete, N. Gelli, and F. Lucarelli, *Physics Letters B* **685**, 258 (2010).
- [15] P. N. Nadtochy, E. G. Ryabov, A. V. Cheredov, and G. D. Adeev, *The European Physical Journal A* **52**, 308 (2016).
- [16] G. La Rana, A. Brondi, R. Moro, E. Vardaci, A. Ordine, A. Boiano, M. Di Meo, A. Scherillo, D. Fabris, M. Lunardon, G. Nebbia, G. Viesti, M. Cinausero, E. Fioretto, G. Prete, N. Gelli, and F. Lucarelli, *The European Physical Journal A - Hadrons and Nuclei* **16**, 199 (2003).
- [17] K. Mazurek, C. Schmitt, P. N. Nadtochy, and A. V. Cheredov, *Phys. Rev. C* **94**, 064602 (2016).
- [18] E. Vardaci, P. N. Nadtochy, A. Di Nitto, A. Brondi, G. La Rana, R. Moro, P. K. Rath, M. Ashaduzzaman, E. M. Kozulin, G. N. Knyazheva, I. M. Itkis, M. Cinausero, G. Prete, D. Fabris, G. Montagnoli, and N. Gelli, *Phys. Rev. C* **92**, 034610 (2015).
- [19] A. Di Nitto, E. Vardaci, A. Brondi, G. La Rana, M. Cinausero, N. Gelli, R. Moro, P. N. Nadtochy, G. Prete, and A. Vanzanella, *Phys. Rev. C* **93**, 044602 (2016).
- [20] E. Fioretto, M. Cinausero, M. Giacchini, M. Lollo, G. Prete, R. Burch, M. Caldogno, D. Fabris, M. Lunardon, G. Nebbia, G. Viesti, A. Boiano, A. Brondi, G. L. Rana, R. Moro, A. Ordine, E. Vardaci, A. Zaghi, N. Gelli, and F. Lucarelli, *IEEE Transactions on Nuclear Science* **44**, 1017 (1997).
- [21] S. Beghini, C. Signorini, S. Lunardi, M. Morando, G. Fortuna, A. Stefanini, W. Meczynski, and R. Pengo, *Nuclear Instruments and Methods in Physics Research Section A: Accelerators, Spectrometers, Detectors and Associated Equipment* **239**, 585 (1985).
- [22] A. Gavron, *Phys. Rev. C* **21**, 230 (1980).
- [23] A. J. Sierk, *Phys. Rev. C* **33**, 2039 (1986).
- [24] R. Moro, A. Brondi, N. Gelli, M. Barbui, A. Boiano, M. Cinausero, A. Di Nitto, D. Fabris, E. Fioretto, G. La Rana, F. Lucarelli, M. Lunardon, G. Montagnoli, A. Ordine, G. Prete, V. Rizzi, M. Trotta, and E. Vardaci, *The European Physical Journal A* **48**, 159 (2012).
- [25] T. Hüyük, A. Di Nitto, G. Jaworski, A. Gadea, J. Javier Valiente-Dobón, J. Nyberg, M. Palacz, P.-A. Söderström, R. Jose Aliaga-Varea, G. de Angelis, A. Ataç, J. Collado, C. Domingo-Pardo, F. J. Egea, N. Erduran, S. Ertürk, G. de France, R. Gadea, V. González, V. Herrero-Bosch, A. Kaşkaş, V. Modamio, M. Moszynski, E. Sanchis, A. Triossi, and R. Wadsworth, *The European Physical Journal A* **52**, 55 (2016).
- [26] N. Bohr and J. A. Wheeler, *Phys. Rev.* **56**, 426 (1939).
- [27] J. Gomez del Campo and R. G. Stockstad, *Oak Ridge National Laboratory Report No. TM7295* (1981).
- [28] M. Brack, J. Damgaard, A. S. Jensen, H. C. Pauli, V. M. Strutinsky, and C. Y. Wong, *Rev. Mod. Phys.* **44**, 320 (1972).
- [29] P. Paul and M. Thoennessen, *Annual Review of Nuclear and Particle Science* **44**, 65 (1994).
- [30] M. Thoennessen and G. F. Bertsch, *Phys. Rev. Lett.* **71**, 4303 (1993).
- [31] P. N. Nadtochy, A. Brondi, A. Di Nitto, G. La Rana, R. Moro, E. Vardaci, A. Ordine, A. Boiano, M. Cinausero, G. Prete, V. Rizzi, N. Gelli, and F. Lucarelli, *EPJ Web of Conferences* **2**, 08003 (2010).
- [32] J. Huizenga and G. Igo, *Nuclear Physics* **29**, 462 (1962).
- [33] F. G. Perey, *Phys. Rev.* **131**, 745 (1963).
- [34] D. Wilmore and P. Hodgson, *Nuclear Physics* **55**, 673 (1964).
- [35] L. C. Vaz and J. M. Alexander, *Zeitschrift für Physik A Atoms and Nuclei* **318**, 231 (1984).